

Supplemental Data

TFIIH and P-TEFb Coordinate Transcription with Capping Enzyme Recruitment at Specific Genes in Fission Yeast

Laia Viladevall, Courtney V. St. Amour, Adam Rosebrock, Susanne Schneider, Chao Zhang, Jasmina J. Allen, Kevan M. Shokat, Beate Schwer, Janet K. Leatherwood, and Robert P. Fisher

Supplemental Experimental Procedures

General Yeast Methods

Strains used in this study are listed in Supplemental Table 1. Cells were grown at 30°C in yeast extract medium with supplements (YES). *S. pombe* cell culture, transformation, tetrad dissection and sporulation were performed according to standard methods (Moreno et al., 1991). Mutagenesis and tagging were done by homology-directed gene targeting (Bähler et al., 1998). For biochemical assays, cells in mid-log phase were lysed in homogenization buffer (HB: 25 mM HEPES [pH 7.4], 0.1% (v/v) Triton X-100, 150 mM NaCl, 2 mM EDTA, 50 mM NaF, 0.1 mM Na₃VO₄, 4 µg/ml leupeptin, 1.3 mM benzamidine, 1 mM PMSF, 1 mM DTT, complete protease inhibitor cocktail [Roche]).

Immunological Methods

Immunoblotting was performed with antibodies specific for: unphosphorylated CTD (8WG16, Covance); Ser5-phosphorylated CTD (polyclonal, Bethyl; or H14, Covance); Ser2-phosphorylated CTD (Bethyl); CTD doubly phosphorylated at Ser2 and Ser5 (H5, Covance); Myc epitope (9E10, Covance); HA epitope (sc-7392, Santa Cruz Biotechnology) or calmodulin-binding protein (CBP) portion of the TAP tag (C16T, Upstate; or polyclonal, Millipore).

Microarray and qRT-PCR Analysis

For microarray experiments, total RNA was extracted from snap-frozen cells as directed (Ambion RiboPure Yeast, Austin, TX). Synthesis of labeled cDNA was performed as described (Oliva et al., 2005). Two-color hybridization was performed on custom manufactured arrays composed of spotted long PCR probes covering the 3' region of all predicted *S. pombe* ORFs. Detailed information on array composition, manufacture, and processing is available at ArrayExpress: www.ebi.ac.uk/ArrayExpress under accession numbers A-MEXP-1284 and A-MEXP-1280.

Statistical Analysis

Data were normalized within the Bioconductor package (Gentleman et al., 2004) by fitting to a normal + exponential convolution model (Smyth, 2005), and intensity dependent bias was removed by loess correction. All spots except those manually flagged at time of scanning were included in further analysis. A linear model was fit to replicate spots present on each array; fits for repeated arrays were performed separately. Significance of differential expression was determined by an empirical Bayes statistic (Smyth, 2004).

Pearson correlations of \log_2 fold-change values from these contrasts were clustered as described previously (Eisen et al., 1998) and visualized with JavaTreeView (<http://jtreeview.sf.net>).

Supplemental References

- Bähler, J., Wu, J. Q., Longtine, M. S., Shah, N. G., McKenzie, A., 3rd, Steever, A. B., Wach, A., Philippsen, P., and Pringle, J. R. (1998). Heterologous modules for efficient and versatile PCR-based gene targeting in *Schizosaccharomyces pombe*. *Yeast* 14, 943-951.
- Eisen, M. B., Spellman, P. T., Brown, P. O., and Botstein, D. (1998). Cluster analysis and display of genome-wide expression patterns. *Proc Natl Acad Sci U S A* 95, 14863-14868.
- Gentleman, R. C., Carey, V. J., Bates, D. M., Bolstad, B., Dettling, M., Dudoit, S., Ellis, B., Gautier, L., Ge, Y., Gentry, J., et al. (2004). Bioconductor: open software development for computational biology and bioinformatics. *Genome Biol* 5, R80.
- Guiguen, A., Soutourina, J., Dewez, M., Tafforeau, L., Dieu, M., Raes, M., Vandehaute, J., Werner, M., and Hermand, D. (2007). Recruitment of P-TEFb (Cdk9-Pch1) to chromatin by the cap-methyl transferase Pcm1 in fission yeast. *Embo J* 26, 1552-1559.
- Moreno, S., Klar, A., and Nurse, P. (1991). Molecular genetic analysis of fission yeast *Schizosaccharomyces pombe*. *Methods Enzymol* 194, 795-823.
- Oliva, A., Rosebrock, A., Ferrezuelo, F., Pyne, S., Chen, H., Skiena, S., Fitcher, B., and Leatherwood, J. (2005). The cell cycle-regulated genes of *Schizosaccharomyces pombe*. *PLoS Biol* 3, e225.
- Smyth, G. K. (2004). Linear models and empirical bayes methods for assessing differential expression in microarray experiments. *Stat Appl Genet Mol Biol* 3, Article3.
- Smyth, G. K. (2005). Limma: linear models for microarray data, In *Bioinformatics and Computational Biology Solutions Using R and Bioconductor*, R. Gentleman, V. Carey, S. Dudoit, R. Irizarry, and W. Huber, eds. (New York: Springer), pp. 397-420.

Table S1. Strains Used in this Study

| Strain | Genotype | Source |
|--------|--|--------------------------------|
| JS78 | <i>leu1-32 ura4-D18 his3-D1 ade6-M210 h+</i> | Saiz, Fisher 2002 2002 2002 |
| LV7 | <i>cdk9^{T120G}::KanMX6 leu1-32 ura4-D18 his3-D1 ade6-M210 h+</i> | This work |
| LV77 | <i>mcs6^{L87G}::KanMX6 leu1-32 ura4-D18 his3-D1 ade6-M216 h-</i> | This work |
| SG2 | <i>mcs6^{L87G}-HA3::kanMX4 leu1-32 ura4-D18 his3-D1 ade6-M216 h-</i> | S Garrett |
| CS118 | <i>lsk1^{F353G}::kanMX6 leu1-32 ura4-D18 his3-D1 ade6-M216 h-</i> | This work |
| HD6-51 | <i>cdk9-13myc::kanMX6 leu1-32 ura4-D18 his3-D1 ade6-M210 h+</i> | Pei et al. 2006 |
| SUS3 | <i>pcm1-2XTAP::kanMX leu1-32 ura4-D18 his3-D1 ade6-M21X h-</i> | S Schneider |
| CS80 | <i>pmh1-2XTAP::kanMX6 leu1-32 ura4-D18 his3-D1 ade6-M210 h+</i> | This work |
| CS146 | <i>pcm1-13myc::kanMX6 leu1-32 ura4-D18 his3-D1 ade6-M210 h+</i> | This work |
| CS111 | <i>spt5-13myc::kanMX6 leu1-32 ura4-D18 his3-D1 ade6-M210 h+</i> | This work |
| LV42 | <i>cdk9^{T120G}::KanMX6 mcs6^{L87G}-HA3:: kanMX4 leu1-32 ura4-D18 his3-D1 ade6-M21X h-</i> | This work |
| CS63 | <i>cdk9^{T120G}::KanMX6 pcm1-TAP::kanMX leu1-32 ura4-D18 his3-D1 ade6-M210 h+</i> | This work |
| CS165 | <i>cdk9^{T120G}::KanMX6 pcm1-13myc::kanMX6 leu1-32 ura4-D18 his3 D1 ade6-M21X h-/ h+</i> | This work |
| CS112 | <i>cdk9^{T120G}::KanMX6 spt5-13myc::kanMX6 leu1-32 ura4-D18 his3-D1 ade6-M21X h+</i> | This work |
| CS141 | <i>mcs6^{L87G}::KanMX6 pmh1-2XTAP::kanMX6 leu1-32 ura4-D18 his3 D1 ade6-M21X h-</i> | This work |
| CS142 | <i>mcs6^{L87G}::KanMX6 pmh1-HA3::kanMX6 leu1-32 ura4-D18 his3 D1 ade6-M21X h-/ h+</i> | This work |
| CS103 | <i>mcs6^{L87G}::KanMX6 cdk9-13myc::kanMX6 leu1-32 ura4-D18 his3-D1 ade6-M21X h-</i> | This work |
| LV81 | <i>mcs6^{L87G}::KanMX6 pcm1-13myc::kanMX6 leu1-32 ura4-D18 his3-D1 ade6-M21X h-/ h+</i> | This work |
| CS155 | <i>mcs6^{L87G}::KanMX6 spt5-13myc::kanMX6 leu1-32 ura4-D18 his3-D1 ade6-M21X h-</i> | This work |
| CS54 | <i>cdk9-13myc::kanMX6 pcm1-2XTAP::kanMX leu1-32 ura4-D18 his3-D1 ade6-M21X h+</i> | This work |
| LV40 | <i>cdk9^{T120G}::KanMX6 rpb1(1-1640)::natR leu1-32 ura4-D18 his3-D1 ade6-M21X h-/ h+</i> | This work |
| LV101 | <i>cdk9^{T120G}::KanMX6 spt5(1-800)::KanMX leu1-32 ura4-D18 his3-D1 ade6-M21X h-/ h+</i> | This work |
| LV105 | <i>mcs6^{L87G}::KanMX6 spt5(1-800)::KanMX leu1-32 ura4-D18 his3-D1 ade6-M21X h-/ h+</i> | This work |
| LV78 | <i>mcs6^{L87G}::KanMX6 cdk9-13myc::kanMX6 pmh1-2XTAP::kanMX6 leu1-32 ura4-D18 his3 D1 ade6-M21X h-/ h+</i> | This work |

Table S2. Primer Pairs Used for ChIP

| Amplicon | Size (bp) | Position | Forward primer | Reverse Primer |
|---------------|-----------|-----------|-----------------------|------------------------|
| <i>aro1_1</i> | 131 | -117/+13 | AGCTCTCATGAATTTTAGC | GATTCGTTTGACATCTTGC |
| <i>aro1_2</i> | 143 | +736/+879 | CTCAATTCGTAATAAGTGTG | AATTGCAACACACTCTCCATG |
| <i>eng1_1</i> | 118 | -160/-278 | GGGAAATCTTGAAACCCAAG | GCTGCTTAAGGATTTATTAGAC |
| <i>eng1_2</i> | 85 | -45/+63 | CTCTGTCTTTCCTTTTAGTCA | ATATAAAAGAACGTAAATAGG |
| <i>eng1_3</i> | 111 | +133/+244 | CCAATGTTTTCGACTCTGTTG | TAGGGGAGCTCAAGCTGTCA |
| <i>eng1_4</i> | 103 | +560/+663 | GACTGAGGGTATGGCCGTTA | AGTACCCGGCACTTCGACA |
| <i>cdc25</i> | 102 | -86/+663 | CTCCATTAGTTCTTTTTGC | TGTTGGTAAAGGAAAGTGAAG |

Figure S1. Finding a Selective Inhibitor of $Mcs6^{as}$ and $Cdk9^{as}$

The dose-response of wild-type (JS78), $cdk9^{as}$ (LV7) and $mcs6^{as-3HA}$ (SG2) cells to different PP1 derivatives. Cells were grown in YES in 96-well microtitre dishes and growth was quantified relative to a DMSO-treated control as in Figure 2A, but inhibitor concentrations were plotted in logarithmic scale. Note: the $cdk9^{T120G}$ allele we integrated did not contain an epitope tag; the resulting strain was resistant to 1-NM-PP1, which was reported to inhibit growth of a $cdk9^{T120G}$ -TAP strain (Guiguen et al., 2007). We directly compared $mcs6^{L87G}$ (strain LV81) with $mcs6^{L87G-3HA}$ (strain SG2) in the same assay, and detected a difference in IC_{50} of 3-MB-PP1 (~40 μ M versus ~30 μ M, respectively), consistent with an effect of the tag as a possible explanation of the discrepancy.

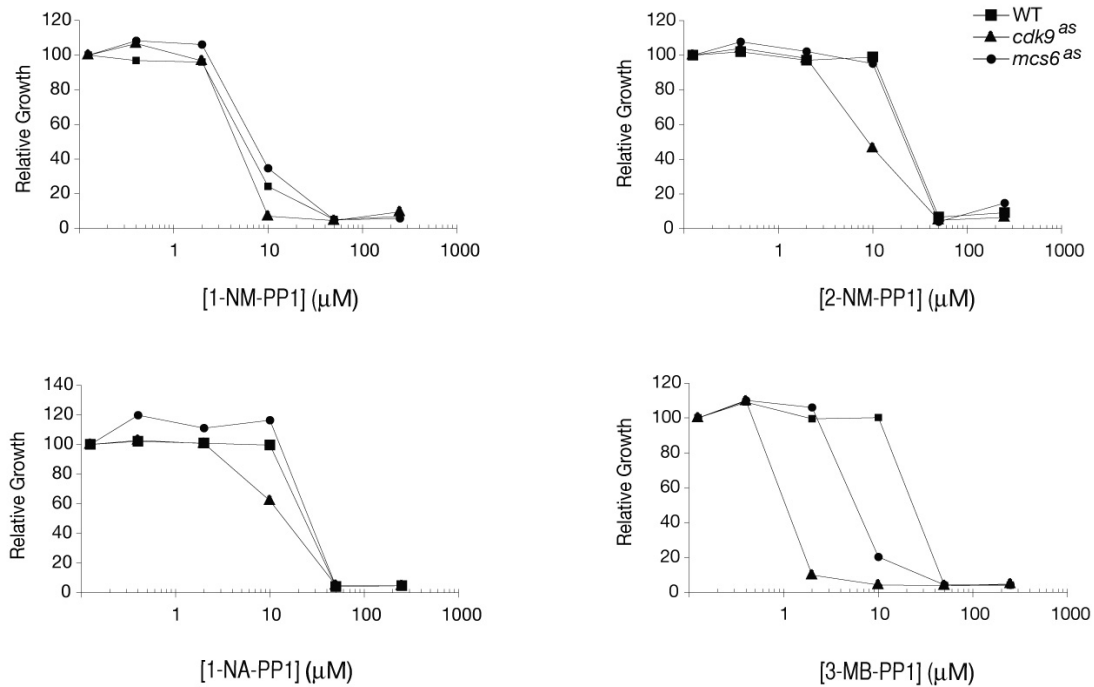


Figure S2. Dose-dependent effects of Mcs6, Cdk9 and Lsk1 inhibition on Pol II phosphorylation

Exponentially growing cells of same strains as in Figure 1C were treated for 1 hr with indicated concentrations of 3-MB-PP1. Extracts were analyzed by immunoblotting with P-Ser5, P-Ser2 and 8WG16 antibodies.

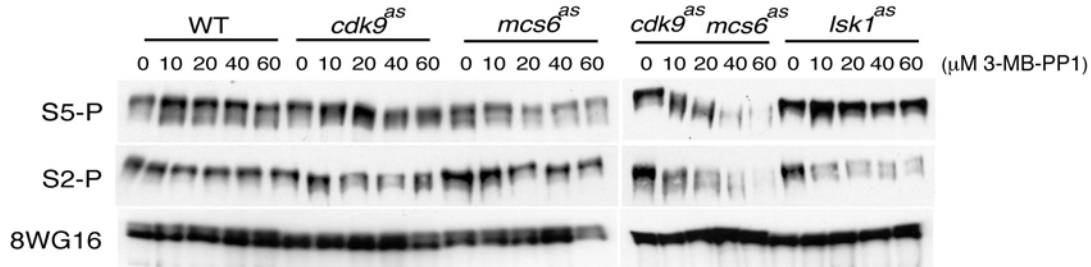


Figure S3. Mcs6 inactivation does not destabilize TFIIF or interfere with PIC assembly

Occupancy of Mcs6 at *eng1⁺* and *aro1⁺* in *mcs6^{as}-3HA* (SG2) cells treated for 1 hr with 20 μM 3-MB-PP1 or DMSO. Error bars denote S.E.M in triplicate measurements.

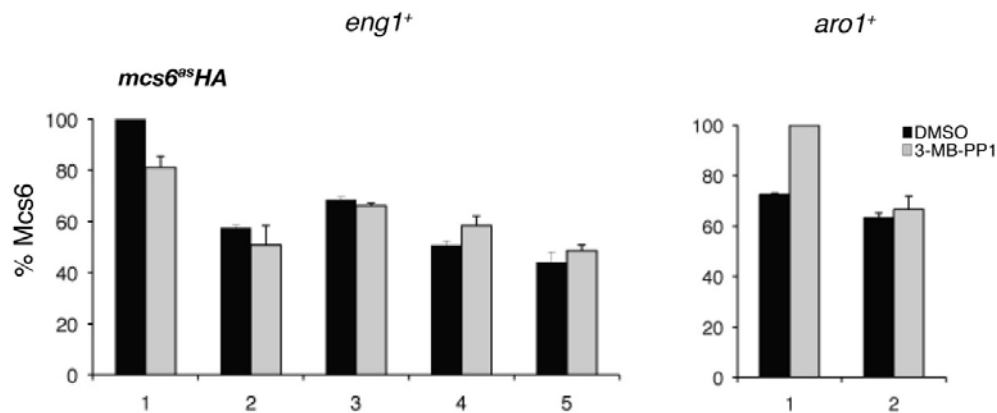


Figure S4. Mcs6 inhibition causes a defect in recruitment of Cdk9/Pcm1 complex at a CDK-dependent gene

ChIP signals of Cdk9, Pcm1 or Pol II at *eng1*⁺ and *aro1*⁺ after 1-hr treatment with 20 μM 3-MB-PP1 or DMSO in indicated strains. Error bars denote S.E.M in triplicate measurements.

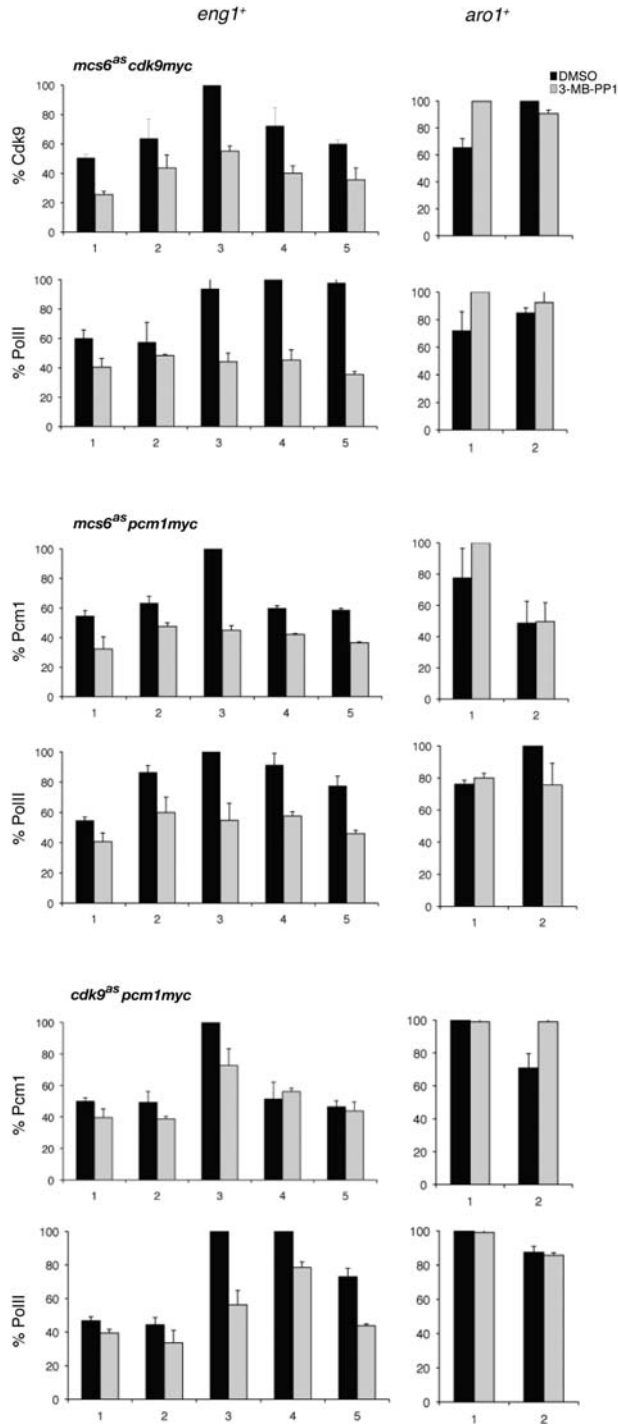


Figure S5. 3-MB-PP1 does not affect Cdk9 and Pcm1 occupancy in wild-type cells *cdk9-myc* (HD6-51) and *pcm1-myc* (CS146) cells were treated for 15 min with 40 μ M 3-MB-PP1 or DMSO (A), or for 1 hr with 20 μ M 3-MB-PP1 or DMSO (B). ChIP signals for Cdk9, Pcm1 or Pol II at *eng1⁺* and *aro1⁺* genes were measured for each condition as indicated. Error bars denote S.E.M in triplicate measurements.

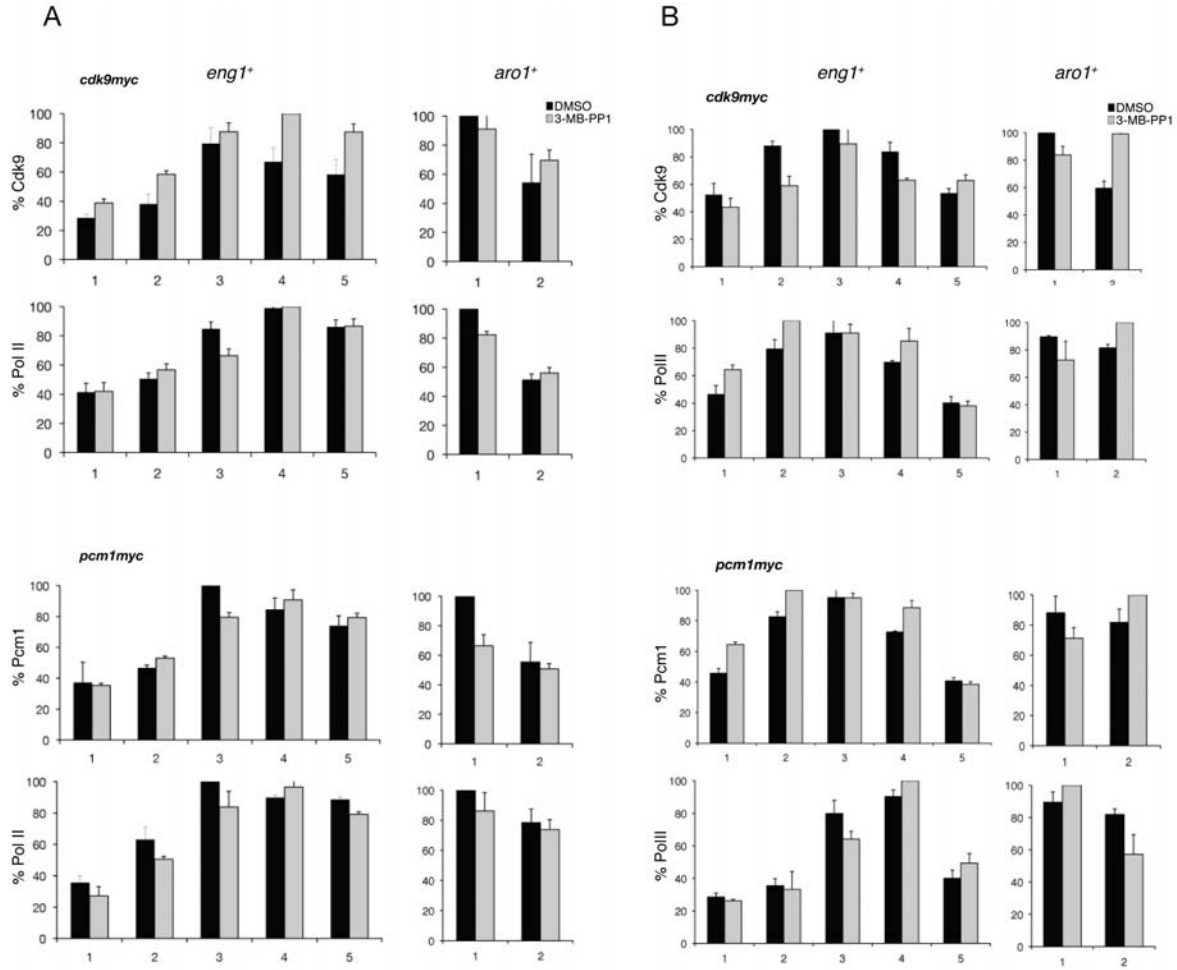


Figure S6. Mcs6 Inhibition Does Not Affect Cdk9/Pcm1 Complex Integrity

Cdk9-myc and Pcm1-TAP were immunoprecipitated as in Figure 5C. Inhibition of Mcs6, in an *mcs6^{as} cdk9-13Myc* strain (CS103), did not affect the Cdk9-Pcm1 interaction.

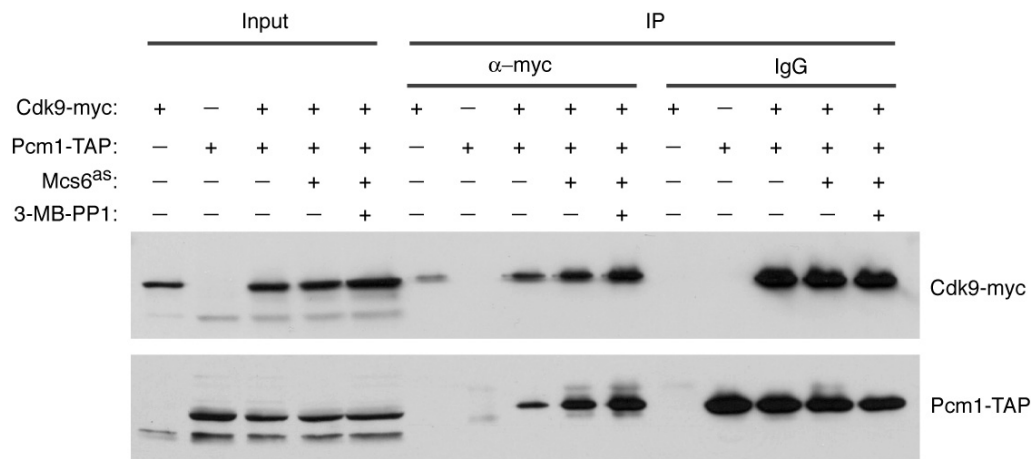


Figure S7. Inhibition of Msc6 or Cdk9 Enhances Chromatin Association of Spt5.

(A) Spt5 and Pol II occupancy at *eng1*⁺ and *aro1*⁺ in *mcs6*^{ΔS} *spt5myc* (top), *cdk9*^{ΔS} *spt5myc* (middle) mutants and isogenic wild-type strain (bottom) after 15-min treatment with 40 μM 3-MB-PP1 or DMSO. Error bars denote S.E.M in triplicate measurements.

(B) Same as (A) after 1 hr with 20 μM 3-MB-PP1 or DMSO.

(C) Ratio of signals of Spt5 (20 μM 3-MB-PP1 versus DMSO) to Pol II (20 μM 3-MB-PP1 versus DMSO) from ChIP signals represented in (B).

